

Energy Landscapes for Digital Alchemy

John W. R. Morgan^{*,†} and Sharon C. Glotzer^{‡,¶,§}

[†]*University Chemical Laboratories, Lensfield Road, Cambridge CB2 1EW, UK*

[‡]*Department of Chemical Engineering, University of Michigan, Ann Arbor, USA*

[¶]*Department of Materials Science and Engineering, University of Michigan, Ann Arbor,
USA*

[§]*Biointerfaces Institute, University of Michigan, Ann Arbor, USA,*

E-mail: jwrm2@cam.ac.uk

Abstract

We apply energy landscape methods to digital alchemy, defining a system in which the parameters of the potential are treated as degrees of freedom. Using geometrical optimisation, we locate minima and transition states on the landscape for small clusters. We show that it is easy to find the parameters that give the lowest energy minimum, and that the distribution of minima on the alchemical landscape is concentrated in particular areas. We also conclude that the alchemical landscape is more frustrated, in terms of competition between low energy structures separated by high barriers. Transition states on the alchemical landscape are classified by whether they become minima or transition states when the potential parameters are fixed. Those that become minima have a significant alchemical component, while those that remain as transition states can be characterised mainly in terms of atomic displacements.

1 Introduction

A fundamental challenge in colloidal science is posed by the vast array of possible colloids that can be made.^{1–4} The complexity and time required to physically manufacture designer particles means that is not possible to fully explore the parameter space. Computer simulations allow a greater throughput and there has been some success using the energy landscape approach⁵ to predict assembly pathways and structures for colloidal systems.^{6–8}

Typically, a computational investigation involves defining a potential with a set of parameters to describe the system. Simulations may be run at different values of the parameters to explore the behaviour or locate a region of parameter space supporting behaviour of interest. An alternative approach is to allow the parameters themselves to vary. This technique is known as digital alchemy, as it involves changing the nature of the particles modelled. The model parameters are already included in the potential energy function. These parameters become variables rather than fixed quantities and can be changed by step taking algorithms in Monte Carlo simulations or evolved dynamically in molecular dynamics simulations, in a thermodynamically consistent way.⁹ Previous work has mostly focused on changing the particle shape, but the approach can be applied much more generally. By exploring a landscape with such extended degrees of freedom, it may be possible to locate the optimal parameters for a particular structure much more quickly and to identify features that favour a particular target.^{9–11}

Following previous work⁹ we investigate the potential energy landscape of the oscillating pair potential (OPP).¹² Originally developed in the context of metal alloys, this potential displays interesting phase behaviour, including an icosahedral quasicrystal.¹³ Here we exploit it as a toy potential with two adjustable parameters that displays many local minima in the alchemical landscape. We define the alchemical landscape to mean the potential energy landscape including both the particle Cartesian coordinates and the alchemical coordinates as variables. As proof of concept, we survey the alchemical landscape for small clusters of particles, locating energy minima and transition states, and compare with fixed parameter

landscapes in various ranges. We also make some observations on the nature of transition states on the alchemical landscape.

2 Methods

2.1 Oscillating Pair Potential

The form of the OPP is

$$V(\mathbf{r}) = \sum_{i \neq j} V_{ij}(\mathbf{r}_i, \mathbf{r}_j),$$

$$V_{ij}(\mathbf{r}_i, \mathbf{r}_j) = \frac{\epsilon\sigma^{15}}{r_{ij}^{15}} + \frac{\epsilon\sigma^3}{r_{ij}^3} \cos\left(k\left(\frac{r_{ij}}{\sigma} - 1.25\right) - \phi\right), \quad (1)$$

where r_{ij} is the distance between a pair of particles and the sum runs over all pairs of particles. $V_{ij}(\mathbf{r}_i, \mathbf{r}_j)$ is the pair potential, ϵ is the unit of energy and σ is the unit of distance. The alchemical parameters are k and ϕ . k represents a frequency and controls the spacing between wells: a higher value of k means there are more wells in the potential. k was restricted to the range $5 < k < 20$ using a harmonic repulsion away from forbidden regions

$$V_k(k) = \begin{cases} \epsilon k_{rep} (k - 5)^2, & \text{if } k < 5, \\ \epsilon k_{rep} (k - 20)^2, & \text{if } k > 20, \\ 0, & \text{otherwise.} \end{cases} \quad (2)$$

A value of $k_{rep} = 10^4$ was sufficient for the harmonic repulsion constant. Any minima or transition states located outside the acceptable k range were ignored. ϕ represents a phase. ϕ is periodic over the range $0 \leq \phi < 2\pi$, so no constraints were necessary.

Usually, a cutoff is not required in the potential when modelling clusters. Here, however, the potential continues to oscillate even at very long range, so without a cutoff there are actually an infinite number of wells and an infinite number of local potential energy minima. To avoid this scenario, a cutoff was introduced. The Stoddard-Ford procedure¹⁴ proved to

be unsuitable, as the continuing oscillations could make the gradient far from zero at the cutoff distance, introducing very large changes to the potential. Instead the XPLOR^{15,16} smoothing function was used, with the smoothing beginning at $r_{ij} = 2.5$ and the potential and gradient going smoothly to 0 at $r_{ij} = 3$.

2.2 Generating Databases

To generate a database of minima and transition states, basin-hopping (BH) global optimisation^{5,17–19} as implemented in **GMIN**²⁰ was first run to locate the global potential energy minimum and other low-lying minima. These minima were used as end points for transition state searches using the doubly-nudged^{21–23} elastic band^{24–28} algorithm and eigenvector following²⁹ as implemented in **OPTIM**.³⁰ A **PATHSAMPLE**³¹ database was initialised from these connections and expanded using additional double-ended and single-ended^{29,32,33} transition state searches. The resulting database constitutes a kinetic transition network, from which phenomenological rates and thermodynamic properties can be extracted.³⁴

2.3 Digital Alchemy

During alchemical simulations, the potential parameters k and ϕ are allowed to vary and are optimised in the same manner as particle coordinates. The BH and transition state search procedures do not depend on the nature of the variables being optimised, so no modifications were needed. The BH procedure requires the first derivatives of the pair potential with respect to the parameters, which are

$$\begin{aligned} \frac{\partial V_{ij}}{\partial k} &= -\epsilon \sin \left(k \left(\frac{r_{ij}}{\sigma} - 1 \right) - \phi \right) \left(\frac{r_{ij}}{\sigma} - 1 \right) \frac{\sigma^3}{r_{ij}^3}, \\ \frac{\partial V_{ij}}{\partial \phi} &= \epsilon \sin \left(k \left(\frac{r_{ij}}{\sigma} - 1 \right) - \phi \right) \frac{\sigma^3}{r_{ij}^3}. \end{aligned} \quad (3)$$

Normal mode analysis and some transition state search algorithms benefit from analytical second derivatives, which include the mixed derivatives with respect to position and potential

parameters. These derivatives are also straightforward; the explicit results are omitted for brevity. Appropriate products with the XPLOR smoothing function and its derivatives must also be included.

The potential energy surface does not depend on the temperature or the mass of the particles. Hence questions about what mass is associated with the alchemical degrees of freedom and whether their response to temperature is the same as for particle Cartesian degrees of freedom are avoided. However, for calculating free energies, these questions must be addressed. In this work, the main results do not depend on this choice, but we also calculate heat capacities as a post-processing tool only, using the same mass and temperature for the alchemical degrees of freedom as for the atomic coordinates.

2.4 Frustration Index

A frustration index can be used to quantify the amount of frustration present in a landscape,^{35,36} defined in terms of low energy minima separated by high barriers. Here we use a recently developed index based on the barrier heights between the global minimum and the other minima.³⁷ The definition is

$$\tilde{f}(T) = \sum_{\alpha \neq g\text{min}} \frac{p_{\alpha}^{\text{eq}}(T)}{1 - p_{g\text{min}}^{\text{eq}}(T)} \left(\frac{V_{\alpha}^{\dagger} - V_{\text{gmin}}}{V_{\alpha} - V_{\text{gmin}}} \right), \quad (4)$$

where the sum runs over all minima other than the global minimum, p_{α}^{eq} is the equilibrium occupation probability of minimum α , V_{α} is the potential energy of minimum α , and V_{α}^{\dagger} is the potential energy of the highest transition state on the lowest energy path between minimum α and the global minimum.

3 Results

We sought the smallest cluster of particles that would display interesting behaviour when the alchemical landscape was explored. Four particles can all be nearest neighbours (in a

regular tetrahedral arrangement), and the alchemical parameters then adjust to make the nearest neighbour well as deep as possible. There are only a very few minima, corresponding to the k and ϕ combinations that give a minimum in the well depth with respect to changing k and ϕ .

Five particles cannot all be nearest neighbours. Non-nearest neighbour interactions can still be optimised when they are at a distance corresponding to a different well in the OPP potential. With alchemical variation of k and ϕ , these potential parameters can also adjust to make a particular distance more favourable, leading to more complicated behaviour than for the four particle cluster.

A database of minima and transition states was created for the five particle cluster, including the alchemical degrees of freedom. Table I shows the size of the database and the energy of the lowest minimum found. The database is not complete, as evidenced by the absence of pathways between all pairs of minima, but the difficulty of discovering new minima and transition states suggests that the majority of structures have been located. In fact, the only pathway between a pair of minima may consist of transition states and intermediate minima that lie outside the permitted k range, so even with a complete database, the network may not be fully connected.

Table I: k and ϕ values for selected databases, with the number of minima and transition states in those databases, the number of minima in the largest connected component, and the energy of the lowest minimum found. The reason for the selection of these k and ϕ values is summarised in the final column.

k	ϕ	N_{\min}	N_{ts}	N_{con}	E_{\min}/ϵ	description
alchemical		6760	10386	2492	-4.9693	
6.00	1.00	61	714	58	-1.9792	low density
8.74	4.37	2931	12691	1184	-4.9693	global minimum
19.75	5.00	458977	489497	221179	-4.6385	high density

The distribution of minima throughout k and ϕ space is shown in figure 1. It is striking that most minima occur within a small region of alchemical space, with most combinations of parameters having no minima at all. Most minima occur around the ϕ value that gives

the deepest nearest-neighbour well and at higher k values, meaning there are more wells in the potential and more possible distances between pairs of particles.

Databases of minima and transition states at fixed alchemical parameters were also generated. A landscape with fixed alchemical parameters is a slice through the full alchemical landscape. Their parameters and characteristics are summarised in table I, with plots of the potential in figure 2. Three alchemical points were selected, corresponding to the global minimum from the alchemical database, a region with a low density of minima, and a region with a high density of minima. In all cases, the global minimum was a trigonal bipyramidal (point group D_{3h}), differing only in the distances between particles, which adjust to match the distance for the deepest well in the potential.

The fixed parameter database in the low density region is unsurprisingly small, and we note that there are no alchemical minima at these parameter values. At high alchemical minima density, the number of minima with fixed parameters is much larger than the total number of alchemical minima. Allowing alchemical variation can reduce the number of minima and transition states on the landscape, as most structures that are stationary points with the parameters fixed are not stationary points when they are allowed to vary.

This result stands in contrast to the usual behaviour when adding more degrees of freedom by adding more particles, where the number of minima tends to increase exponentially on increasing the number of particles.³⁸⁻⁴⁰ Most minima at fixed parameter values will not be minima in the extended space, as changes to the potential can usually be made that decrease the energy. Conversely, on adding a new particle to a system, minima will often exist with very similar pair distances to structures before the addition. The main difference, then, is that changing the alchemical parameters affects all the pair distances together.

The landscapes for the four systems are summarised in the disconnectivity graphs shown in figure 3.^{41,42} Apart from the very different numbers of minima, the structures of the graphs are fairly similar, corresponding to “palm tree” funnelled landscapes.⁴² The alchemical system is most similar to the high density system. Taken in conjunction with the density distribution

in figure 1, it is clear that the contributions from the high density region are dominating alchemical space.

To compare the landscapes more quantitatively, we have calculated the frustration indices for the four systems, shown in figure 4. To facilitate comparison, the temperature has been scaled for each system by T_m , the value at which the heat capacity has a maximum. Heat capacities were calculated within the harmonic superposition approximation.⁴³ A mass must be assigned for each degree of freedom and it was not obvious what mass to use for the alchemical variables. Unit mass was arbitrarily chosen, as for the atomic coordinates. Therefore, care should be taken to not overinterpret the value of the frustration index, but we can make some general observations, which were found to be robust to variation of the fictitious mass.

The alchemical database is very frustrated at low temperatures, indicating relatively high barriers between the global minimum and other minima with significant occupation probabilities. The energies and alchemical parameters of the ten lowest energy alchemical minima are shown in table II, demonstrating that the low energy minima are widely separated in alchemical space. The pathways between these minima must cross unfavourable alchemical regions, giving high barriers. The other three systems exhibit lower frustration. At high temperatures, the frustration disappears for the alchemical system as the barriers become thermally accessible. Due to the higher frustration, we expect self-assembly on this alchemical landscape to be more difficult than on the fixed parameter landscapes, especially at low temperature. The system would become trapped in local minima with thermally inaccessible barriers preventing progress towards the global minimum.

All stationary points on the alchemical landscape must be stationary points on the corresponding fixed parameter landscape when the parameters are equal to those of the alchemical minimum. The inverse is not necessarily true: a stationary point on a fixed landscape is unlikely to remain a stationary point when the parameters are allowed to vary. An alchemical minimum must be a fixed parameter minimum, but an alchemical transition state could

Table II: The energies, k and ϕ values of the ten lowest energy alchemical minima. The minima are widely separated in alchemical space.

Energy / ϵ	k	ϕ
−4.9693	8.74	4.37
−4.9690	17.42	5.60
−4.7570	13.40	4.96
−4.6784	15.38	5.24
−4.5811	8.57	4.33
−4.5798	17.02	5.50
−4.5518	15.45	5.14
−4.4844	17.43	5.40
−4.4436	16.20	5.26
−4.4314	18.19	5.32

remain a transition state or become a minimum once the parameters are fixed. The second case indicates that the reaction coordinate at the transition state has significant components for the alchemical degrees of freedom. This situation is analogous to a martensitic transition, in which the reaction coordinate involves a change in lattice parameters rather than particle coordinates.⁴⁴

Of the 10386 alchemical transition states in the database, 346 became minima when the parameters were fixed. Although it may seem sensible to call these ‘pure alchemical transitions’, the reaction coordinate may not be precisely localised on the alchemical degrees of freedom. We can quantify the ‘alchemical content’ of a transition state by taking the dot product of the reaction coordinate with a normalised vector parallel to the alchemical degrees of freedom. The reaction coordinate is the normalised eigenvector corresponding to the single negative Hessian eigenvalue at the transition state.⁴⁵ In table III we present the root mean square (RMS) k and ϕ content for both classes of alchemical transition state. While it is clear that those alchemical transition states that become minima tend to have a much greater alchemical component in the reaction coordinate, and that k tends to have a greater contribution than ϕ , they are not purely alchemical. Conversely, those transition states that remain as transition states tend to have a very small alchemical component and are almost purely described in terms of Cartesian coordinate displacements.

Table III: RMS k and ϕ contributions to the reaction coordinate at alchemical transition states, for those transition states that become minima when the parameters are fixed, and for those that remain transition states.

Transition state becomes...	k contribution	ϕ contribution
Transition state	0.0396	0.019
Minimum	0.497	0.154

4 Conclusions

We have explored the potential energy landscape of small clusters in an extended system where the parameters of the potential are also variables. As proof of concept, we have shown that geometrical approaches for exploring the landscape are feasible and allow rapid location of the global minimum.

We have compared some properties of the alchemical system to systems with fixed parameters, showing that there is a significant difference between introducing alchemical degrees of freedom compared to adding another particle. Although in this particular case, it seems that high frustration on the alchemical landscape would hinder self-assembly in an experimental system, that is no barrier to basin-hopping global optimisation and theoretical prediction of the best parameters is possible.

We also analyse characteristics of pathways on the alchemical surface, showing that some are almost purely describable in terms of atomic displacements, while others contain a significant amount of alchemical character.

We expect that digital alchemy will become an important theoretical tool, as it has general applicability to a wide range of systems. In addition to ongoing work on the shape of colloids, we envision coarse-grained potentials with variable parameters, ‘floppy-bodies’ - previously rigid bodies allowed to change shape in a restricted manner - and protein mutations.

Conflicts of Interest

There are no conflicts of interest to declare.

Acknowledgement

The authors thank James Proctor and Pengji Zhou for comments on the original manuscript. Financial support was provided by the United Kingdom Engineering and Physical Sciences Research Council (EPSRC). Data may be accessed at <<http://doi.org/10.5281/zenodo.3256234>>

References

- (1) Zhang, Z.; Glotzer, S. C. Self-assembly of patchy particles. *Nano Lett.* **2004**, *4*, 1407–1413.
- (2) Glotzer, S. C.; Solomon, M. J. Anisotropy of building blocks and their assembly into complex structures. *Nat. Mater.* **2007**, *6*, 557–562.
- (3) Pawar, A. B.; Kretzschmar, I. Fabrication, assembly, and application of patchy particles. *Macromol. Rapid Commun.* **2007**, *31*, 150–168.
- (4) Sacanna, S.; Pine, D. J. Shape-anisotropic colloids: Building blocks for complex assemblies. *Curr. Opin. Colloid Interface Sci.* **2011**, *16*, 96–105.
- (5) Wales, D. J. *Energy landscapes*; Cambridge University Press, 2003.
- (6) Morgan, J. W. R.; Chakrabarti, D.; Dorsaz, N.; Wales, D. J. Designing a Bernal spiral from patchy colloids. *ACS Nano* **2013**, *7*, 1246–1256.
- (7) Morphew, D.; Chakrabarti, D. Supracolloidal reconfigurable polyhedra via hierarchical self-assembly. *Soft Matter* **2016**, *12*, 9633–9640.
- (8) Fejer, S. N.; Wales, D. J. Design of a kagome lattice from soft anisotropic particles. *Soft Matter* **2015**, *11*, 6663–6668.
- (9) van Anders, G.; Klotsa, D.; Karas, A. S.; Dodd, P. M.; Glotzer, S. C. Digital alchemy for materials design: Colloids and beyond. *ACS Nano* **2015**, *9*, 9542–9553.
- (10) Du, C. X.; van Anders, G.; Newman, R. S.; Glotzer, S. C. Shape-driven solid-solid transitions in colloids. *Proc. Natl. Acad. Sci. USA* **2017**, *114*, E3892–E3899.
- (11) Cersonsky, R. K.; van Anders, G.; Dodd, P. M.; Glotzer, S. C. Relevance of packing to colloidal self-assembly. *Proc. Natl. Acad. Sci. USA* **2018**,

(12) Mihalkovič, M.; Henley, C. L. Empirical oscillating potentials for alloys from ab initio fits and the prediction of quasicrystal-related structures in the Al-Cu-Sc system. *Phys. Rev. B* **2012**, *85*, 092102.

(13) Engel, M.; Damasceno, P. F.; Phillips, C. L.; Glotzer, S. C. Computational self-assembly of a one-component icosahedral quasicrystal. *Nat. Mater.* **2015**, *14*, 109–116.

(14) Stoddard, S. D.; Ford, J. Numerical experiments on the stochastic behavior of a Lennard-Jones gas system. *Phys. Rev. A* **1973**, *8*, 1504–1512.

(15) Anderson, J. A.; Lorenze, C. D.; Travesset, A. General purpose molecular dynamics simulations fully implemented on graphics processing units. *J. Comput. Phys.* **2008**, *227*, 5342–5359.

(16) Glaser, J.; Nguyen, T. D.; Anderson, J. A.; Liu, P.; Spiga, F.; Millan, J. A.; Morse, D. C.; Glotzer, S. C. Strong scaling of general-purpose molecular dynamics simulations on GPUs. *Comput. Phys. Commun.* **2015**, *192*, 97–107.

(17) Li, Z.; Scheraga, H. A. Monte Carlo-minimization approach to the multiple-minima problem in protein folding. *Proc. Natl. Acad. Sci. USA* **1987**, *84*, 6611–6615.

(18) Li, Z.; Scheraga, H. A. Structure and free energy of complex thermodynamic systems. *J. Mol. Struc-Theochem* **1988**, *179*, 333.

(19) Wales, D. J.; Doye, J. P. K. Global optimization by basin-hopping and the lowest energy structures of Lennard-Jones clusters containing up to 110 atoms. *J. Phys. Chem. A* **1997**, *101*, 5111–5116.

(20) Wales, D. J. GMIN: A program for basin-hopping global optimisation. <http://www-wales.ch.cam.ac.uk/software.html>.

(21) Trygubenko, S. A.; Wales, D. J. A doubly nudged elastic band method for finding transition states. *J. Chem. Phys.* **2004**, *120*, 2082–2094.

(22) Trygubenko, S. A.; Wales, D. J. Erratum: A doubly nudged elastic band method for finding transition states [J. Chem. Phys. 120, 2082 (2004)]. *J. Chem. Phys.* **2004**, *120*, 7820–7820.

(23) Sheppard, D.; Terrell, R.; Henkelman, G. Optimization methods for finding minimum energy paths. *J. Chem. Phys.* **2008**, *128*, 134106.

(24) Mills, G.; Jónsson, H. Quantum and thermal effects in H₂ dissociative adsorption: Evaluation of free energy barriers in multidimensional quantum systems. *Phys. Rev. Lett.* **1994**, *72*, 1124–1127.

(25) Mills, G.; Jónsson, H.; Schenter, G. K. Reversible work transition state theory: application to dissociative adsorption of hydrogen. *Surf. Sci.* **1995**, *324*, 305–337.

(26) Jónsson, H.; Mills, G.; Jacobsen, K. W. *Classical and quantum dynamics in condensed phase simulations*; World Scientific: Singapore, 1998.

(27) Henkelman, G.; Uberuaga, B. P.; Jónsson, H. A climbing image nudged elastic band method for finding saddle points and minimum energy paths. *J. Chem. Phys.* **2000**, *113*, 9901–9904.

(28) Henkelman, G.; Jónsson, H. Improved tangent estimate in the nudged elastic band method for finding minimum energy paths and saddle points. *The Journal of Chemical Physics* **2000**, *113*, 9978–9985.

(29) Munro, L. J.; Wales, D. J. Defect migration in crystalline silicon. *Phys. Rev. B* **1999**, *59*, 3969–3980.

(30) Wales, D. J. OPTIM: A Program for optimizing geometries and calculating reaction pathways. <http://www-wales.ch.cam.ac.uk/software.html>.

(31) Wales, D. J. PATHSAMPLE: A program for generating connected stationary point databases and extracting global kinetics. <http://www-wales.ch.cam.ac.uk/software.html>.

(32) Wales, D. J.; Doye, J. P. K.; Miller, M. A.; Mortenson, P. N.; Walsh, T. R. Energy landscapes: From clusters to biomolecules. *Adv. Chem. Phys.* **2000**, *115*, 1–111.

(33) Kumeda, Y.; Wales, D. J.; Munro, L. J. Transition states and rearrangement mechanisms from hybrid eigenvector-following and density functional theory: Application to C₁₀H₁₀ and defect migration in crystalline silicon. *Chem. Phys. Lett.* **2001**, *341*, 185–194.

(34) Wales, D. J. Exploring energy landscapes. *Annu. Rev. Phys. Chem.* **2018**, *69*, 401–425.

(35) Bryangelson, J. D.; Onuchic, J. N.; Soccia, N. D.; Wolynes, P. G. Funnels, pathways, and the energy landscape of protein folding: A synthesis. *Proteins: Struct., Funct., Genet.* **1995**, *21*, 167–195.

(36) Onuchic, J. N.; Luthey-Schulten, Z.; Wolynes, P. G. Theory of protein folding: The energy landscape perspective. *Annu. Rev. Phys. Chem.* **1997**, *48*, 545–600.

(37) de Souza, V. K.; Stevenson, J. D.; Niblett, S. P.; Farrell, J. D.; Wales, D. J. Defining and quantifying frustration in the energy landscape: Applications to atomic and molecular clusters, biomolecules, jammed and glassy systems. *J. Chem. Phys.* **2017**, *146*, 124103.

(38) Stillinger, F. H.; Weber, T. A. Packing structures and transitions in liquids and solids. *Science* **1984**, *225*, 983–989.

(39) Wales, D. J.; Doye, J. P. K. Stationary points and dynamics in high-dimensional systems. *J. Chem. Phys.* **2003**, *119*, 12409–12416.

(40) Morgan, J. W. R.; Wales, D. J. Energy landscapes of planar colloidal clusters. *Nanoscale* **2014**, *6*, 10717–10726.

(41) Becker, O. M.; Karplus, M. The topology of multidimensional potential energy surfaces: theory and application to peptide structure and kinetics. *J. Chem. Phys.* **1997**, *106*, 1495–1517.

(42) Wales, D. J.; Miller, M. A.; Walsh, T. A. Archetypal energy landscapes. *Nature* **1998**, *394*, 758–760.

(43) Wales, D. J. Coexistence in small inert gas clusters. *Mol. Phys.* **1993**, *78*, 151–171.

(44) Patel, J.; Cohen, M. Criterion for the action of applied stress in the martensitic transformation. *Acta Metall.* **1953**, *1*, 531–538.

(45) Murrell, J. N.; Laidler, K. J. Symmetries of activated complexes. *Trans. Faraday Soc.* **1968**, *64*, 371–377.

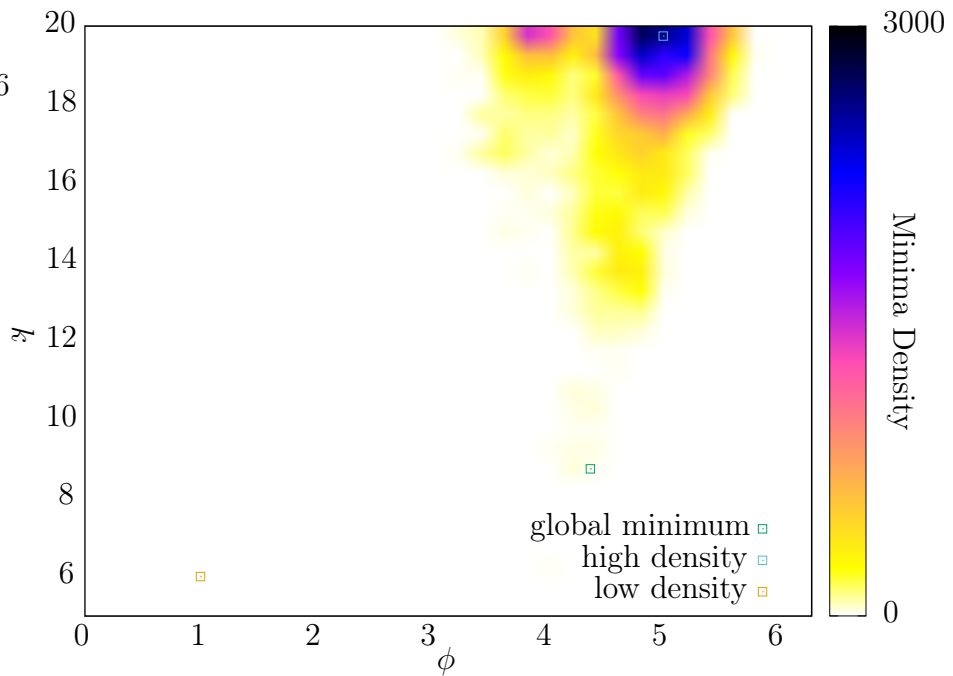


Figure 1: The density of minima as a function of the alchemical parameters k and ϕ . Most of the space has no minima at all. Unit density corresponds to one minimum in an area of one k unit by one ϕ unit. The points chosen for generating fixed parameter databases are also shown.

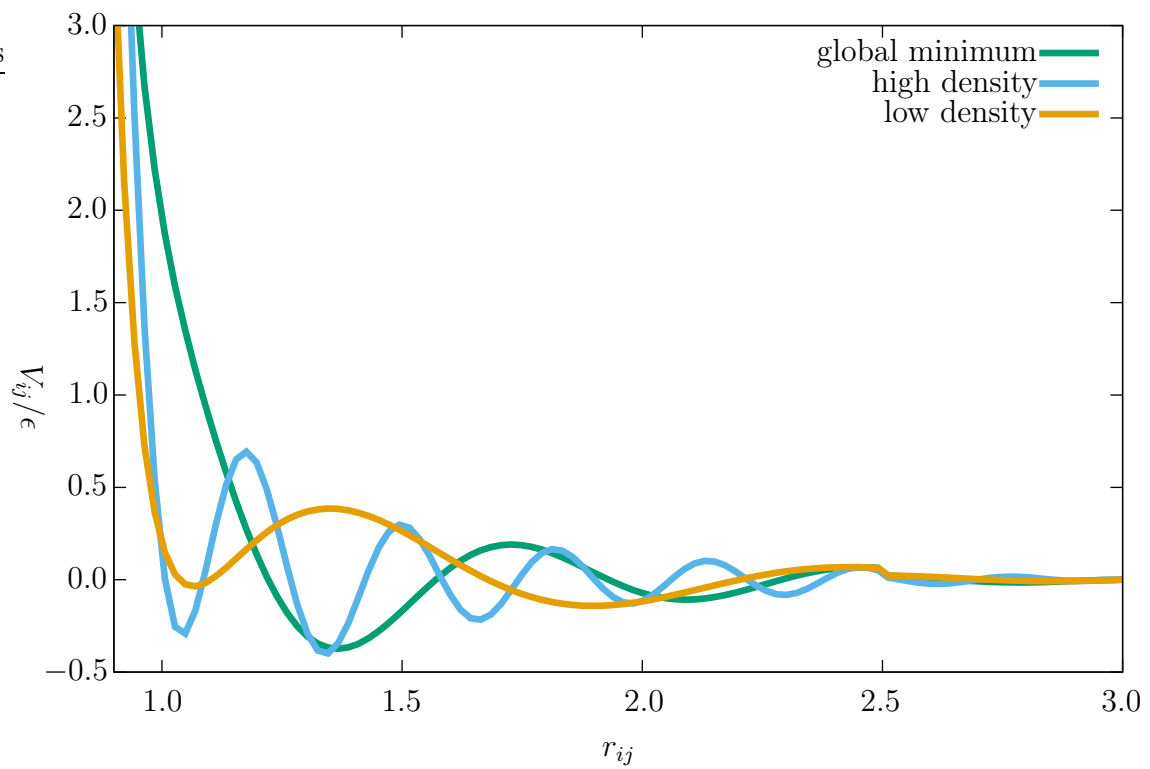


Figure 2: The OPP potential for the three sets of fixed parameters used, as listed in table I.

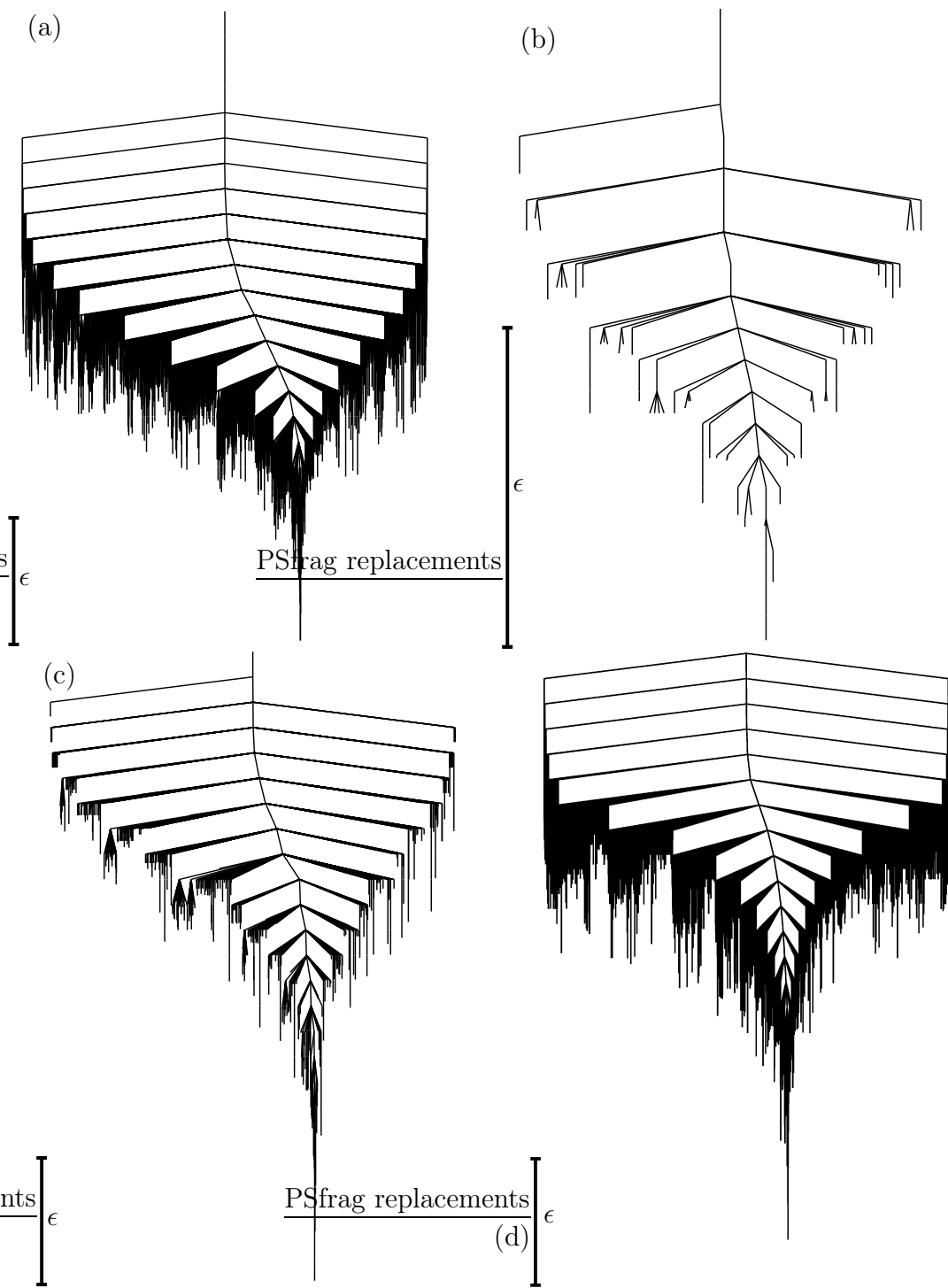


Figure 3: Disconnectivity graphs for the alchemical landscape and the three fixed parameter landscapes, as listed in table I, showing the connected component including the global minimum. (a) The alchemical system. (b) The low density system. (c) The global minimum system. (d) The high density system.

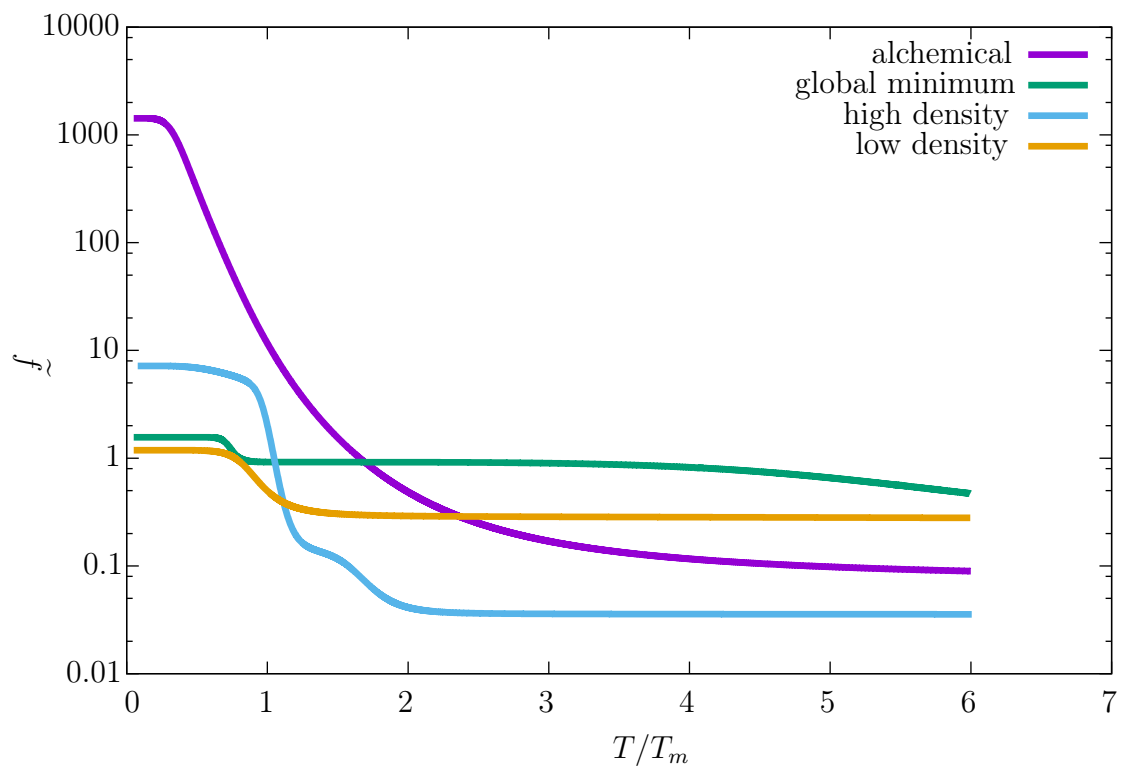


Figure 4: The variation of the frustration indices with temperature for the four databases. The temperature has been scaled by the temperature of the greatest value of the heat capacity, T_m , for each database.

Graphical TOC Entry

